

## Organization of cellulose fibrils in the capsular matrix of *Acidisarcina polymorpha* SBC82<sup>T</sup> identified by synchrotron radiation

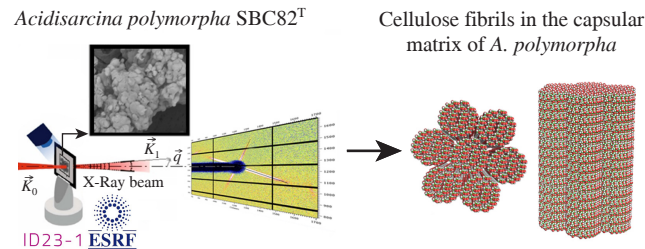
Vladislav V. Kovalenko,<sup>a</sup> Svetlana E. Belova,<sup>b</sup> Ksenia B. Tereshkina,<sup>a</sup> Eduard V. Tereshkin,<sup>a</sup> Yurii F. Krupyanskii<sup>a</sup> and Nataliya G. Loiko<sup>\*b</sup>

<sup>a</sup> N. N. Semenov Federal Research Center for Chemical Physics, Russian Academy of Sciences, 119991 Moscow, Russian Federation. E-mail: vladislavkovalenko785@gmail.com

<sup>b</sup> Federal Research Center 'Fundamentals of Biotechnology' of the Russian Academy of Sciences, 119071 Moscow, Russian Federation. E-mail: loikonat@mail.ru

DOI: 10.71267/mencom.7604

**A structural study of the cellulose-containing capsular matrix of *Acidisarcina polymorpha* SBC82<sup>T</sup> was carried out using synchrotron radiation. Analysis of the diffraction pattern from a 45-day-old population of acidobacteria revealed that the crystalline structure of the capsular matrix, formed by cellulose fibrils with cylindrical symmetry, is well described by a two-dimensional hexagonal lattice. Processing of diffraction data allowed us to calculate the radius of fibrils in the main ( $17.0 \pm 0.5$  Å) and additional ( $10 \pm 5.9$  Å) directions and their mass ratio (9 : 1), as well as to estimate the size of the crystalline domain of the capsules (50 nm).**



**Keywords:** X-ray diffraction, chain molecules, small-angle X-ray scattering, SAXS, wide-angle X-ray scattering, WAXS, *Acidisarcina polymorpha*, cellulose fibrils.

Recently, small-angle X-ray scattering (SAXS) and wide-angle X-ray scattering (WAXS), collectively referred to as SWAXS, have become increasingly popular in structural biology as a way to study the overall shape and state of biological macromolecules.<sup>1</sup> SAXS can be used to determine the radius of gyration, maximum extent, molecular weight and shape of a macromolecule at low resolution, and to model complexes consisting of several macromolecules.<sup>2</sup> SAXS can quantify flexibility and conformational changes in the structure of biopolymers with temporal resolution and, in the presence of fibrous structure, determine the orientation of microfibers.<sup>3,4</sup> WAXS methods are often used to obtain microstructural parameters (periodic structural features as small as 40 Å) of polymers.<sup>5,6</sup>

The advantage of SWAXS is the speed of research, as well as the ability to study extremely small objects, comparable to the size of an X-ray beam, in a native physiological state without special sample preparation.<sup>7</sup> At the same time, the use of SWAXS together with other high-resolution structural methods, such as X-ray crystallography, nuclear magnetic resonance spectroscopy and electron microscopy, multiplies the number of problems solved.<sup>8–10</sup>

Due to the rapidity of data acquisition, SWAXS techniques are widely used to study the structural changes that chain molecules of biopolymers undergo under various types of deformation.<sup>11,12</sup> For example, they have been used to study protein fibrils such as actomyosin<sup>13</sup> and collagen<sup>14–16</sup> or cellulose fibrils of wood.<sup>17,18</sup>

Previously, we successfully applied the SAXS method to analyze the structure of fibrils in cellulose-containing capsules of *Acidisarcina polymorpha* SBC82<sup>T</sup>, a recently described member

of the phylum *Acidobacteriota* isolated from acidic forest-tundra soil (Nadym, Yamalo-Nenets Autonomous Okrug, Russia).<sup>19,20</sup> Colonies of these bacteria on solid agar medium consisted of polymorphic cells organized into bundle- or cluster-like aggregates surrounded by a very large cellulose-containing capsule [Figure 1(a),(b)],<sup>20</sup> which looks like modern nanomaterials.<sup>21</sup> The capsule allows these bacteria to adapt to different habitats and survive in adverse conditions. The SAXS method proved the presence of ordered fibrils in the capsules, with a deviation from parallel arrangement of 3.3°. However, it was not possible to estimate the size of the fibrils themselves in the capsules due to the ambiguity of the interpretation of the diffraction data.

In this work, we continued to investigate the capsule structure of the acidobacterium *A. polymorpha* SBC82<sup>T</sup> using SWAXS methods, focusing on the structure of the capsule layer in areas of high cell aggregation, where individual capsules fused with each other to form a dense biopolymer matrix [Figure 1(c),(d)]. The aim of the research was to evaluate the shape, size and mutual arrangement of cellulose-containing fibrils in the dense biopolymer capsular matrix of the acidobacterium *A. polymorpha* SBC82<sup>T</sup> by analyzing small- and large-angle diffraction scattering patterns.

A sample containing a cluster of encapsulated acidobacterium cells [see Figure 1(c),(d)], which were cultured for 45 days on solid MA20 medium to form a dense biopolymer matrix, was investigated at the synchrotron station ID23-1 of the European Synchrotron Radiation Facility (ESRF). The methodology of the study is presented in detail in Online Supplementary Materials. In most of the obtained diffraction patterns, the diffraction scattering was

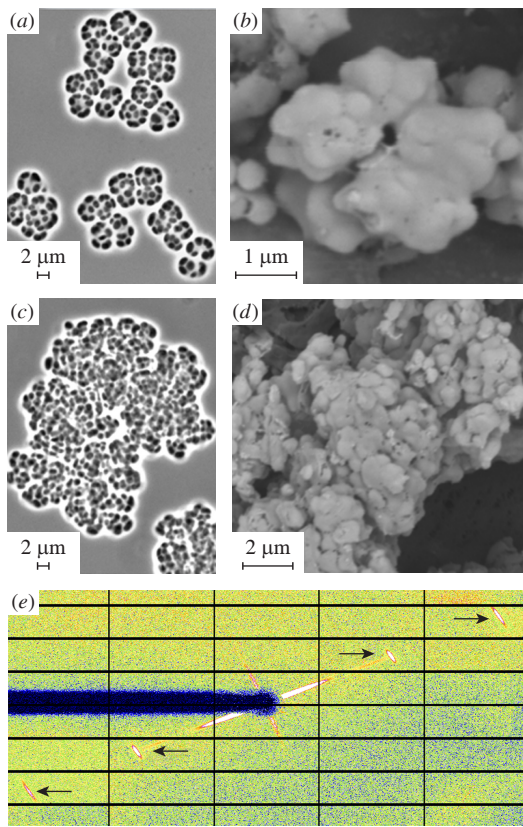


**Figure 1** Images of *A. polymorpha* SBC82<sup>T</sup> culture grown on solid medium for 45 days obtained with (a),(c) Zeiss Axioplan 2 phase contrast microscope using Axiovision 4.2 software and (b),(d) Hitachi TM3000 scanning electron microscope (accelerating voltage 15 kV). (a),(b) Individual cell aggregates stuck together to form (c),(d) a biopolymer matrix. (e) 2D X-ray diffraction scattering pattern of the biopolymer matrix formed by *A. polymorpha* SBC82<sup>T</sup> capsules (ESRF, ID23-1, wavelength 2 Å, beam spot 4 µm, flux  $5 \times 10^{10}$  photons s<sup>-1</sup>, exposure time 5 s per frame, temperature 100 K).

represented by two radial bands, almost perpendicular to each other (the average angle was  $83 \pm 5^\circ$ ), and four diffraction peaks [Figure 1(e)]. They were analyzed at small and large scattering angles. The radial bands in the diffraction pattern indicated a cylindrical symmetry typical of the fibril structure, while the diffraction peaks at high angles indicated a periodic stacking of the fibrils present. The second band indicated the presence of two directions, main and additional, of fibril stacking in the sample.

It should be noted that these diffraction patterns were obtained for samples of adult bacterial culture, in which groups of cells (4–16) are surrounded by a capsule, and the capsules are fused together into a dense matrix [see Figure 1(c),(d)]. A very bright signal from such an object indicated an extreme ordering of the fibrils in it, similar to or even stronger than the ordering of fibrils in wood.<sup>18,19</sup> Apparently, in older cultures, the capsules of acidobacteria perform a role, including mechanical protection of the cells, similar to dense layers of wood protecting the heartwood of the tree. The scattering from younger cells of *A. polymorpha*, as shown earlier,<sup>20</sup> either did not have radial bands at all (in the case of very young cells that had not yet formed a capsule), or was not so intense and did not have an additional perpendicular band.

The analysis of the attenuation intensity pattern along the radial bands located in the main and additional directions allowed us to calculate their radius. The annealing algorithm was applied to select the parameters of the experimental curve (see Online Supplementary Materials). The fibril radii were  $17.0 \pm 0.5$  and  $10 \pm 5.9$  Å, respectively. The large standard deviation of the radius values of the fibrils located in the additional position is due to their high heterogeneity. In this case, not only the radius values were evaluated, but also the fibril size distribution function by radius. Based on

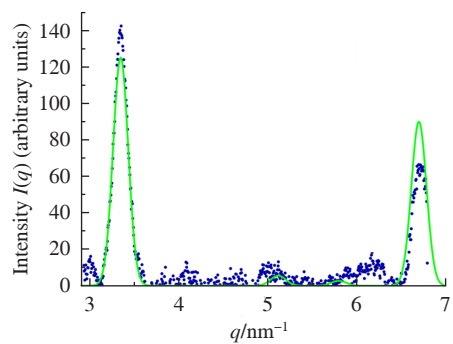


**Figure 2** Averaged intensity distribution over the diffraction peak area for experimental (blue dots) and calculated (green solid line) values.

the integral intensity values along the main and additional fibril directions, it can be assumed that their mass ratio is approximately 9 to 1. Probably, the perpendicular fibrils provide additional rigidity to the capsule structure.

The presence of four diffraction peaks along the equatorial line in the diffraction pattern showed that the fibrils in the capsules are arranged in an ordered manner rather than chaotically. They are well described by a two-dimensional hexagonal lattice perpendicular to the axis of the fibrils forming it. Figure 2<sup>†</sup> shows an almost perfect match between the diffraction data and the model of cellulose fibrils with a hexagonal packing. The distance between the centers of the fibrils in this packing is 37.5 Å. Figure 3<sup>‡</sup> shows a schematic representation of the organization of cellulose fibrils in the intercellular matrix, as well as frontal and lateral views of the atomic model of the arrangement of fibrils.

The width of diffraction maxima along the radial direction is related to the linear size of crystalline domains formed by cellulose fibrils. Using the Scherzer formula<sup>22</sup> for determining the size of crystalline domains, all four diffraction peaks were analyzed. The width of each peak corresponded to a crystalline domain size of 50 nm. Assuming that the ordered domains are also cylindrical in shape, each domain of this size consists of approximately 200 single fibrils with a radius of 17.5 Å. This is in good agreement with the size of the capsule wall estimated from SEM images.

Further calculations showed that the fibrils in the crystalline domain are arranged strictly parallel, with a possible deviation angle of only 5° (see Online Supplementary Materials).

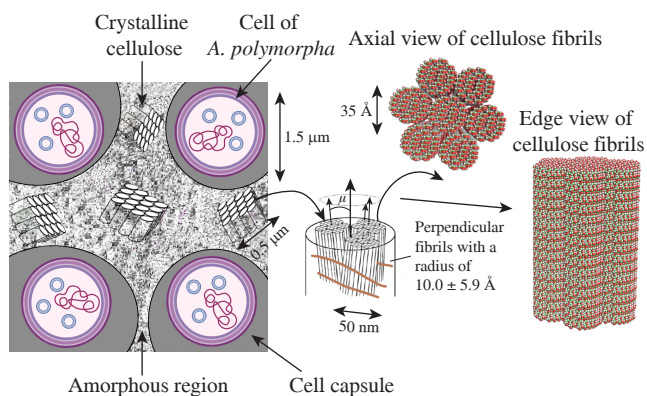


**Figure 3** Schematic representation of the hierarchy of organization of cellulose fibrils in the intercellular matrix. Brown lines represent single fibrils in the additional perpendicular direction.

<sup>†</sup> The calculations were carried out based on the proposed molecular model of cellulose fibrils using the CristalDiffract software (<https://crystalmaker.com/crystaldiffract/index.html>).

<sup>‡</sup> The molecular model of cellulose fibrils was constructed using the Cellulose-Builder ToolKit<sup>23</sup> program and visualized in PyMol (<https://pymol.org>).

In summary, the investigation of the capsular matrix of acidobacterium *A. polymorpha* using synchrotron radiation allowed us to decipher its structure. It was reliably established that it consists of crystalline domains formed by about 200 cellulose-containing fibrils with a radius of  $17.0 \pm 0.5$  Å, very densely (center-to-center distance 37.5 Å) hexagonally packed in one direction (deviation angle 5°), and about 22 perpendicular fibrils with a radius of  $10 \pm 5.9$  Å, connecting the entire structure. This work once again demonstrates the possibility of using SWAXS for successfully solving many problems of structural biology.

This work was supported by the Ministry of Science and Higher Education of the Russian Federation (research topics nos. 102404010 0181-4, 122040800164-6 and 122041100029-2). The computations were performed on the MVS-10P in the Joint Supercomputer Center of the Russian Academy of Sciences. The SEM studies were carried out on the shared research facility ‘Electron Microscopy in Life Sciences’ at Moscow State University (unique equipment ‘Three-Dimensional Electron Microscopy and Spectroscopy’) and using the equipment purchased within the framework of the Moscow State University Development Program. The authors are grateful to ESRF ID23-1 (Grenoble, France) for the opportunity to conduct X-ray experiments.

#### Online Supplementary Materials

Supplementary data associated with this article can be found in the online version at doi: 10.71267/mencom.7604.

#### References

- 1 T. W. Gräwert and D. I. Svergun, *J. Mol. Biol.*, 2020, **432**, 3078; <https://doi.org/10.1016/j.jmb.2020.01.030>.
- 2 H. Imamura and S. Honda, *Int. J. Mol. Sci.*, 2023, **24**, 12042; <https://doi.org/10.3390/ijms241512042>.
- 3 D. Franke, C. M. Jeffries and D. I. Svergun, *Biophys. J.*, 2018, **114**, 2485; <https://doi.org/10.1016/j.bpj.2018.04.018>.
- 4 D. I. Svergun, M. H. J. Koch, P. A. Timmins and R. P. May, *Small Angle X-Ray and Neutron Scattering from Solutions of Biological Macromolecules*, Oxford University Press, Oxford, UK, 2013; <https://doi.org/10.1093/acprof:oso/9780199639533.001.0001>.
- 5 H. Kumar, Siddaramaiah, R. Somashekhar and S. S. Mahesh, *Eur. Polym. J.*, 2007, **43**, 611; <https://doi.org/10.1016/j.eurpolymj.2006.11.004>.
- 6 F. G. Souza, Jr., B. G. Soares, G. L. Mantovani, A. Manjunath, H. Somashekappa, R. Somashekhar and Siddaramaiah, *Polymer*, 2006, **47**, 2163; <https://doi.org/10.1016/j.polymer.2006.01.033>.
- 7 C. D. Putnam, M. Hammel, G. L. Hura and J. A. Tainer, *Q. Rev. Biophys.*, 2007, **40**, 191; <https://doi.org/10.1017/S0033583507004635>.
- 8 N. B. Chinnam, A. Syed, K. H. Burnett, G. L. Hura, J. A. Tainer and S. E. Tsutakawa, in *DNA Damage Responses. Methods in Molecular Biology*, ed. N. Mosammapparast, Humana, New York, 2022, vol. 2444, pp. 43–68; [https://doi.org/10.1007/978-1-0716-2063-2\\_4](https://doi.org/10.1007/978-1-0716-2063-2_4).
- 9 S. E. Tsutakawa, G. L. Hura, K. A. Frankel, P. K. Cooper and J. A. Tainer, *J. Struct. Biol.*, 2007, **158**, 214; <https://doi.org/10.1016/j.jsb.2006.09.008>.
- 10 M. Hammel, D. J. Rosenberg, J. Bierma, G. L. Hura, R. Thapar, S. P. Lees-Miller and J. A. Tainer, *Prog. Biophys. Mol. Biol.*, 2021, **163**, 74; <https://doi.org/10.1016/j.pbiomolbio.2020.09.003>.
- 11 E. Chi, Y. Tang and Z. Wang, *ACS Omega*, 2021, **6**, 11762; <https://doi.org/10.1021/acsomega.1c01365>.
- 12 T. Kamal, S.-Y. Park, M.-C. Choi, Y.-W. Chang, W.-T. Chuang and U.-S. Jeng, *Polymer*, 2012, **53**, 3360; <https://doi.org/10.1016/j.polymer.2012.05.037>.
- 13 M. Priebe, M. Bernhardt, C. Blum, M. Tarantola, E. Bodenschatz and T. Salditt, *Biophys. J.*, 2014, **107**, 2662; <https://doi.org/10.1016/j.bpj.2014.10.027>.
- 14 M. M. Basil-Jones, R. L. Edmonds, S. M. Cooper and R. G. Havercamp, *J. Agric. Food Chem.*, 2011, **59**, 9972; <https://doi.org/10.1021/jf202579b>.
- 15 R. Seidel, A. Gourrier, M. Kerschnitzki, M. Burghammer, P. Fratzl, H. S. Gupta and W. Wagermaier, *Bioinspired, Biomimetic Nanobiomater.*, 2012, **1**, 123; <https://doi.org/10.1680/bbn.11.00014>.
- 16 C. J. Moger, R. Barrett, P. Bleuet, D. A. Bradly, R. E. Ellis, E. M. Green, K. M. Knapp, P. Muthuvelu and C. P. Winlove, *Osteoarthritis and Cartilage*, 2007, **15**, 682; <https://doi.org/10.1016/j.joca.2006.12.006>.
- 17 A. Reiterer, H. F. Jacob, S. E. Stanzl-Tschech and P. Fratzl, *Wood Sci. Technol.*, 1998, **32**, 335; <https://doi.org/10.1007/BF00702790>.
- 18 H. Lichtenegger, A. Reiterer, S. E. Stanzl-Tschech and P. Fratzl, *J. Struct. Biol.*, 1999, **128**, 257; <https://doi.org/10.1006/jsb.1999.4194>.
- 19 S. E. Belova, N. V. Ravin, T. A. Pankratov, A. L. Rakitin, A. A. Ivanova, A. V. Beletsky, A. V. Mardanov, J. S. Sinninghe Damsté and S. N. Dedysh, *Frontiers in Microbiology*, 2018, **9**, 2775; <https://doi.org/10.3389/fmicb.2018.02775>.
- 20 S. E. Belova, D. G. Naumoff, N. E. Suzina, V. V. Kovalenko, N. G. Loiko, V. V. Sorokin and S. N. Dedysh, *Microorganisms*, 2022, **10**, 2253; <https://doi.org/10.3390/microorganisms1012253>.
- 21 V. V. Pavlenko, A. Yu. Zakharov, Z. E. Ayaganov and Z. A. Mansurov, *Russ. Chem. Rev.*, 2024, **93**, RCR5122; <https://doi.org/10.59761/RCR5122>.
- 22 A. L. Patterson, *Phys. Rev.*, 1939, **56**, 978; <https://doi.org/10.1103/PhysRev.56.978>.
- 23 T. C. F. Gomes and M. S. Skaf, *J. Comput. Chem.*, 2012, **33**, 1338; <https://doi.org/10.1002/jcc.22959>.

Received: 2nd September 2024; Com. 24/7604